CHALMERS
UNIVERSITY OF TECHNOLOGY

Surface chemical analysis of copper powder used in additive manufacturing

Citation for the original published paper (version of record):
Bojestig, E., Cao, Y., Nyborg, L. (2020). Surface chemical analysis of copper powder used in additive manufacturing. Surface and Interface Analysis, 52(12): 1104-1110.
http://dx.doi.org/10.1002/sia.6833

Received: 25 October 2019 | Revised: 4 May 2020 | Accepted: 26 May 2020

DOI: 10.1002/sia.6833

ECASIA SPECIAL ISSUE PAPER

SURFACE and INTERFACE ANALYSIS WILEY

Surface chemical analysis of copper powder used in additive manufacturing

Eric Bojestig | Yu Cao | Lars Nyborg

Department of Industrial and Materials Science, Chalmers University of Technology, Gothenburg, Sweden

Correspondence
Eric Bojestig, Department of Industrial and Materials Science, Chalmers University of Technology, Gothenburg, Sweden.
Email: bojestig@chalmers.se

Funding information
Vinnova, Grant/Award Number: 2016-03290

Additive manufacturing (AM) has during years gained significant interest owing to its endless component design possibilities. One of the most popular AM techniques is laser powder bed fusion (LPBF), which selectively melts metal powder layer-by-layer in a chamber with protective argon atmosphere. This technique is attractive for realizing Cu-based products in which the high electrical conductivity of Cu is combined with component design possibilities. The successful use of Cu powder not only poses challenges owing to the high reflectivity and thermal conductivity of Cu but also involves the important concern of controlling the powder surface chemistry since the powder surface constitutes the main source of oxygen. It is of crucial importance to control the oxygen level in order to maintain good electrical conductivity and brazing ability of the AM-fabricated Cu-part. In LPBF, fine spherical powder with size of 10–60 μm is used, providing significant specific surface area, and this powder is also usually recycled several times, and hence, the role of powder surface chemistry is evident. Two kinds of copper powder with purities 99.70 and 99.95 wt% were analysed in both virgin and in used conditions after numerous printing cycles using LPBF. The powder was analysed by X-ray photoelectron spectroscopy (XPS) and scanning electron microscopy (SEM). A clear difference between the two powder grades in terms of surface chemistry was observed. The oxide thickness and bulk oxygen content increased for both powder grades after recycling. The surface oxides under different conditions are identified and the effect of powder purity on the oxide formed is discussed.

KEYWORDS
additive manufacturing (AM), copper oxide, copper powder, surface chemistry, X-ray photoelectron spectroscopy (XPS)

1 | INTRODUCTION

Additive manufacturing (AM) is a collection of manufacturing techniques that manufactures a part layer-by-layer until the final geometry is reached.[1] It provides a unique opportunity to manufacture new, innovative products due to the less restrictive design possibilities and much shorter lead times. One of the most common AM techniques is laser powder bed fusion (LPBF) that utilizes a Nd-YAG laser to melt each nominal 20-μm layer of metal powder with the size range of 10–60 μm^2, along with remelting a number of priorly added layers below. The large specific surface area of the powder means that surface bound oxygen is a source for oxygen carried into the material as

it is built. In order to protect the fine powder when exposed to the elevated temperature close to the built part during the process, a constant flow of protective inert gas (argon) is flooding the build chamber to minimize oxidation and cool the surface. As the LPBF technique matures and the adaptation in the industry expands, the demand for more materials is increasing. Development of an LPBF process for a new alloy is a time-consuming and daunting task.[2] The goal is usually to achieve full density parts with appropriate chemical and mechanical properties. To neglect the role of the powder surface chemistry during this development, process could lead to these goals not be achieved, and it is therefore paramount to be aware of the degradation of powder and ensure that it still can be reused after several cycles.[3,4] Furthermore, powder is usually rather expensive, in the range of 100–200 USD per kilo; hence, the recycling and minimizing the material waste in order to achieve a reasonable manufacturing cost is a main target.

There have previously been many recycling studies performed on different powders for LBPF.[5–7] The joint consensus is that the powder oxygen content may be increased after each printing cycle and thus also associated with the increase of the oxide thickness. How this will affect the material and mechanical properties varies between materials. However, even if the properties are little affected, keeping the oxygen content within certain levels is desirable to attain reproducible and predictable properties within specifications. Nevertheless, the limit for oxygen pick-up and how to evaluate the utilization boundary of the reused powder is still under discussion.

There is interest to manufacture copper parts with LPBF due to the high electric and thermal conductivity.[8] However, the low laser absorption and high thermal conductivity make it problematic to create good, well-defined melt pools.[9] Attempts to manufacture copper parts with LPBF have been done by either printing in a standard machine with tailored material or changing the laser source to one with shorter wave length to increase the absorption rate or to one with much higher power.[10–12] To the knowledge of the authors, there are no published results with full density parts. Due to this, no one have yet prioritized to examine how the copper powder degrades during the process. In a later stage, the oxygen content of the printed part will also affect the capability of brazing. Not being able to do this would severely limit the application.

In order to investigate the LPBF process effect on the powder morphology and surface chemistry for pure copper powder with two different nominal purities grades, 99.70 and 99.95 wt%, the analysis of virgin powder and powder reused several cycles was carried out by means of X-ray photoelectron spectroscopy (XPS) and scanning electron microscope (SEM) and correlated with bulk chemical analyses of total oxygen in order to depict the role of powder surface condition and purity.

2 | MATERIALS AND METHODS

In this study, two different powder purity grades of Cu were used: 99.70 and 99.95 wt%, hereafter called 99.70 and 99.95 grades. All printing were performed in the LPBF machine of type EOS M290 with a protective atmosphere of argon. Additionally, the powders were sieved between each print. The 99.70 grade powder was recycled approximately 10 times, and the 99.95 grade powder was recycled five times. The surface chemistry was studied by means of a PHI VersaProbe III XPS instrument using monochromatized AlK_α (1486.6 eV) X-ray source with beam size of 100 × 1400 μm and power of 100 W. Multiple particles were covered in the XPS analysis. The acquisition conditions were 26 eV pass energy and 0.1 eV/step for region spectra. The recorded photoelectrons peaks were curved fitted to obtain the contribution corresponding to the different chemical states of the elements present. The energy calibration was done using Cu, Ag and Au standards in accordance with ISO 15742:2010. The C 1s peak from adventitious C located at 285 eV was used as energy scale reference. Apparent compositions were retrieved by converting the measured XPS peak intensities determined from the peak areas assuming Shirley background using standard sensitivity factors provided by the PHI Multipak software. The depth profiling was carried out by successive ion etchings and XPS analyses using pass energy of 69 eV. An Ar ion beam of 2 keV energy was applied with raster size of 5 × 5 mm and beam current of 7 mA. The oxide thickness was defined as the depth where the intensity of oxygen decreases half. The etch rate calibrated under these conditions on a flat Ta_2O_5 sample with known overlayer thickness is 1.1 nm/min. The powder shape was not accounted for. Considering these two facts, thickness measures quoted should be viewed as approximate on an absolute scale, but differences between the powder grades can consistently be depicted. The LEO Gemini 1500 FEG-SEM with an in-lens detector was used for assessment of the powder morphology. The inert gas fusion technique was used to determine the total oxygen content.[13]

3 | RESULTS AND DISCUSSION

A clear difference in the powder morphology can be seen for the 99.70 grade before and after recycling; see Figure 1. The 99.95 grade powder was not as severely degraded, but still, some areas of oxide formation were observed. This could be partly a result of the fact that the 99.95 grade powder was not recycled as many times as the 99.70 grade and the lack of available oxygen in the build chamber. The XPS depth profiles from all powders investigated are presented in Figure 2. The purpose here was to compare the oxide thickness under different conditions and to examine the enrichment of element, so only apparent composition was provided. As a surface contamination, C was not included in the profiles. In the case of virgin 99.95 grade powder, O concentration decreased shortly after etching, as shown in Figure 2B. The oxide thickness estimated as the depth when the intensity of O decreased half its initial intensity was 2 nm. Recycling made the O profile less steep (Figure 2A), and the thickness of the oxide increased to 15 nm, as summarized in Table 1. For the 99.70 grade, similarly, the measured oxide thickness increased substantially after recycling from 15 to 30 nm. The similar trend could be observed for the total oxygen content, from 1340 to 1520 ppm for 99.70 grade

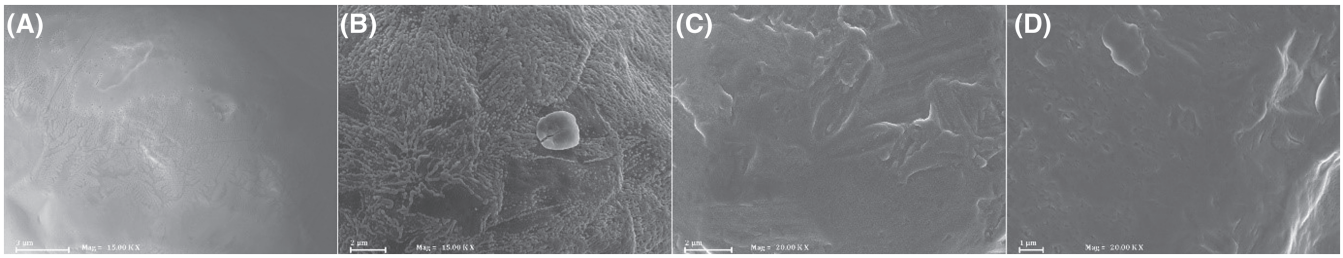

FIGURE 1 Scanning electron microscope images representing the four different powders used in this study in virgin state and after several cycles in the laser powder bed fusion process. (A) 99.70% virgin, (B) 99.70% used, (C) 99.95% virgin, and (D) 99.95% used

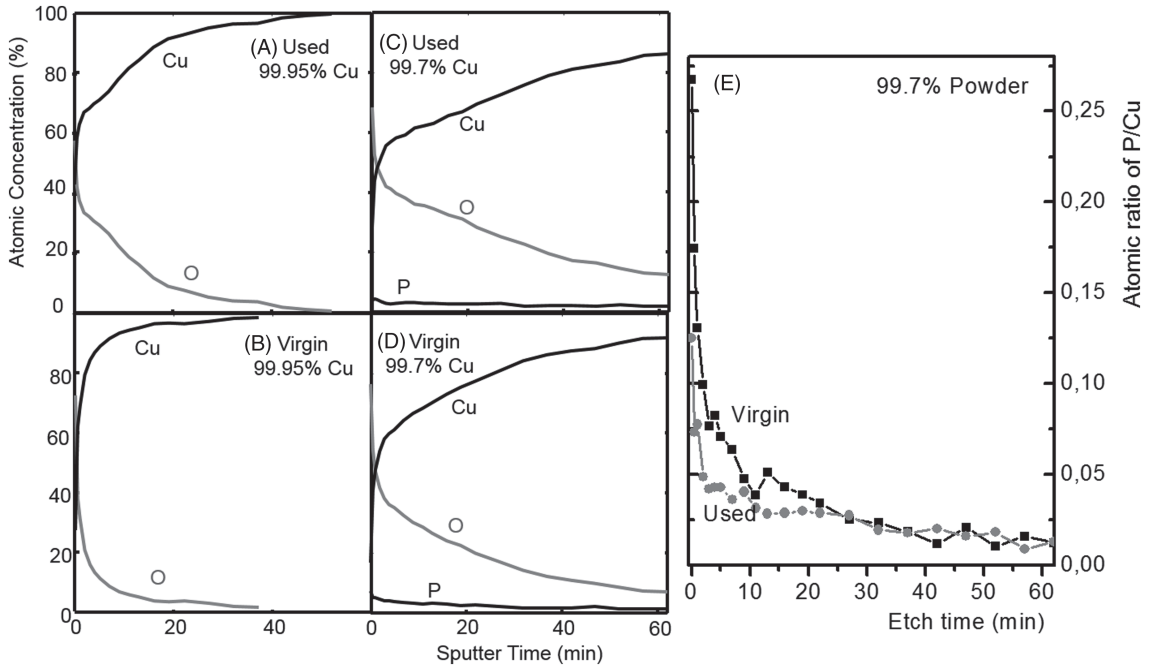

FIGURE 2 Depth profiles from the powders studied (A–D) and atomic ratio of P/Cu of virgin and used 99.70% Cu. C was excluded in the profiles. Etch rate was 1.1 nm/min calibrated on Ta_2O_5

TABLE 1 Total oxygen content, oxide thickness and surface atomic ratio P/Cu for the different powder grades

	99.70% Virgin	99.70% Used	99.95% Virgin	99.95% Used
Total oxygen content (ppm)	1340	1520	124	419
Apparent oxide thickness (nm)	15	30	2	15
Surface atomic ratio P/Cu	0.26	0.12	-	-

and from 124 to 419 ppm for 99.95 grade powder, as presented in Table 1. Hence, there is a clear match between the result of the XPS analyses with total oxygen. Even after recycling, the oxygen content of 99.95 grade was much lower than that of the virgin 99.70 grade powder. This could imply that the 99.95 grade powder can be used for more cycles than 99.70 grade, hence providing lower overall manufacturing cost.

For the 99.70 grade, P in a few atomic per cent was observed on the surface of both virgin and used powder; see Table 2. The atomic ratio of P/Cu was found to be 0.26 for virgin 99.70 grade powder and 0.12 for the recycled state. Figure 2E gives the variation of this ratio as a function of depth. Enrichment of P in the surface region was clearly observed, the extent of which was reduced by recycling. It is known that P has stronger affinity with O, leading to the observed enrichment and higher oxygen concentration at the surface for the 99.70 grade; see Table 2.

TABLE 2 Apparent surface composition (at%)

Sample	C	O	Cu	P
Virgin 99.95	43.8	33.8	22.4	-
Used 99.95	48.5	30.4	21.1	-
Virgin 99.70	40.8	40.1	15.2	3.9
Used 99.70	44.5	37.0	16.4	2.1

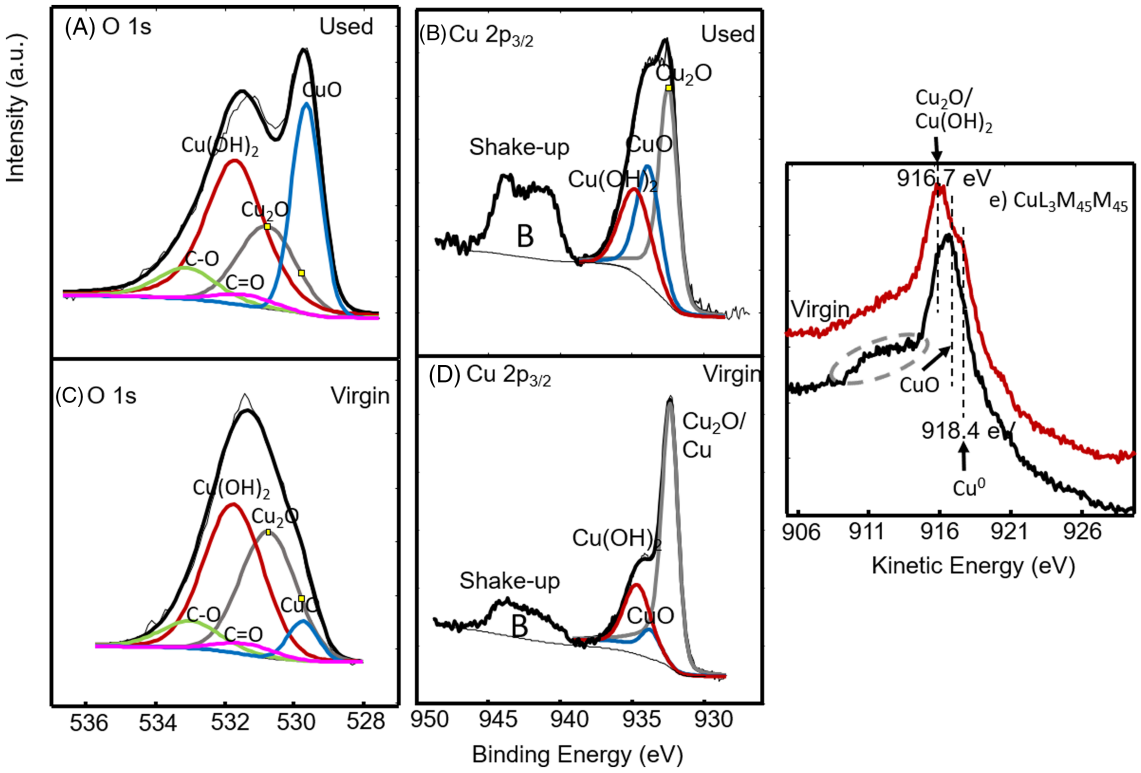

FIGURE 3 XPS core level spectra of Cu $2p_{3/2}$, O 1s and Auger Cu $L_3M_{45}M_{45}$ peaks of virgin and used 99.95% Cu

The XPS core level spectra of Cu $2p_{3/2}$ and O 1s spectra from both as-received and recycled 99.95 grade powder are shown in Figure 3. In the virgin condition (Figure 3D), the main Cu $2p_{3/2}$ peak is located at 932.5 eV, indicating the presence of Cu_2O and/or metallic Cu. To identify the corresponding chemical states, Auger Cu $L_3M_{45}M_{45}$ peak was also recorded, as exhibited in Figure 3E. A shoulder at kinetic energy of 918.4 eV for virgin powder indicated the presence of metallic Cu while the peak at 916.7 eV represented Cu_2O and $Cu(OH)_2$. The observation of metallic Cu was consistent with the small overall apparent oxide thickness of 2 nm, which allows for the penetration of photoelectrons and Auger electrons of Cu from metallic state through the oxide layer. Besides Cu_2O and metallic Cu, curve fitting of Cu $2p_{3/2}$ (Figure 3D) revealed the coexistence of $Cu(OH)_2$ and a small portion of CuO, which are located at ~934.8 and 933.9 eV, respectively. The quantification results are given in Table 3. Curve fitting of O 1s peak (Figure 3C) gave the three oxide components at 529.7 eV for CuO, 530.7 eV for Cu_2O and 531.8 eV for $Cu(OH)_2$, respectively. The contribution of components C–O (533 eV) and C═O (531.4 eV) in Figure 3A,C was associated with adventitious carbon at the surface. After recycling, significant increase of CuO fraction was observed, as revealed by curve fitting of both Cu $2p_{3/2}$ and O 1s in Figure 3 and Table 3. A doublet shake-up structure with increase in intensity on the high binding energy side (marked as B in Figure 3B) provided further evidence for this. It is known the shake-up satellite is entirely from Cu^{2+}. The intensity ratio of the main Cu $2p_{3/2}$ emission line and this satellite have been reported to be 1.57 for $Cu(OH)_2$ and 1.89 for CuO,[14] respectively. For the 99.95 grade powder, recycling increses the ratio from 0.23 to 0.37, as shown in Table 3, being consistent with the increased CuO fraction. This was confirmed again by Cu $L_3M_{45}M_{45}$ Auger peak in Figure 3E. Not only the peak position was shifted, but also a hump (in circle) at high BE

TABLE 3 Intensity ratio of the main Cu $2p_{3/2}$ line and shake-up satellite and atomic per cent of different Cu species at the surface obtained by curve fitting

Sample	Intensity ratio of the main Cu $2P_{3/2}$ line and shake-up satellite	Cu_2O	CuO	$CU(OH)_2$	$CU_3(PO_4)_2$
Virgin 99.95% Cu	0.23	71.1%[a]	5.97%	22.9%	-
Used 99.95% CU	0.37	46.1%	29.2%	24.7%	-
Virgin 99.70% Cu	0.29	62.5%	-	11.6%	25.9%
Used 99.70% Cu	0.25	70.18%	-	18.3%	11.5%

[a]Metallic Cu is included in this value for vigin 99.95% Cu.

side, characteristic of CuO, was observed. In summary, the surface oxides on 99.95 grade powder consisted of Cu_2O, CuO and $Cu(OH)_2$, and recycling increased the fraction of CuO considerably.

The XPS core level spectra of Cu $2p_{3/2}$, O 1s and P 2p spectra and Auger Cu $L_3M_{45}M_{45}$ from both as-received and recycled 99.70 grade are shown in Figure 4. The enrichment of P at the surface region was evident. The main Auger Cu $L_3M_{45}M_{45}$ peak for both powder variants was located at kinetic energy 916.7 eV, suggesting the absence of metallic Cu and the dominance of Cu_2O + $Cu(OH)_2$ (Figure 4C). Curve fitting of Cu $2p_{3/2}$ and O 1s indicated that Cu was mainly in the chemical state of $Cu(OH)_2$, Cu_2O and Cu-phosphate with in latter case Cu $2p_{3/2}$ being located at 935.1 eV while P2p and O 1s being located at 133.4 and 531.4 eV, respectively. Most likely it is in the form of orthophosphate - $Cu_3(PO_4)_2$. Similar binding energy values have been reported by some researchers.[15–17] The formation of phosphate explains the observed higher oxygen concentration for this grade, as shown in Table 2. The CuO was not observed anymore, leading to the reduced intensity ratio of the main Cu $2p_{3/2}$ line and shake-up satellite compared with the 99.95 grade. When comparing these two powder grades, one major difference was the amount of phosphasphate. For the 99.95 grade, no P was found at all, while the Cu bond in phosphate contributed to 25.9% and 11.5% of the Cu $2p_{3/2}$ intensity for virgin and reused 99.95 grade powder, respectively (Table 3). Decrease of phosphate by recycling was accompanied by an increase of Cu_2O and $Cu(OH)_2$. The possible clustering, as well as the potential evaporation during recycling, was expected to make the enrichment of P in phosphate form less evident. These events probably explained the morphology change by recycling as revealed in Figure 1A,B.

Thermodynamic calculations by Magnusson et al. have revealed that copper phosphates have a higher stability than copper oxides at low oxygen activities.[18] With increasing oxygen activity, the metal matrix may, however, oxidize and form Cu_2O, leading to the coexistence of Cu_2O and copper phosphate when oxidizing phosphorus deoxidized copper. At even higher partial pressure of oxygen, CuO becomes stable as well. In the absence of P, the oxygen activity required for the formation of CuO is significantly lower. These mentioned thermodynamic calculations explain the coexistence of Cu_2O and CuO in the surface region of 99.95 grade powder. For 99.70 grade powder containing P, coexisting with Cu-phosphate, the dominant oxide is instead Cu_2O while $Cu(OH)_2$ was only observed at the utmost surface.

Compared with 99.70 grade powder, the 99.95 grade powder showed higher CuO and $Cu(OH)_2$ surface content. This suggests significantly improved passivated surface condition, which is also consistent with the much smaller overall apparent oxide thickness of 2 nm compared with that of 15 nm for the 99.70 grade powder in virgin condition.

With respect to the virgin powder, recycling the 99.70 grade for 10 times led to an increase of oxide thickness by ~15 nm (from 15

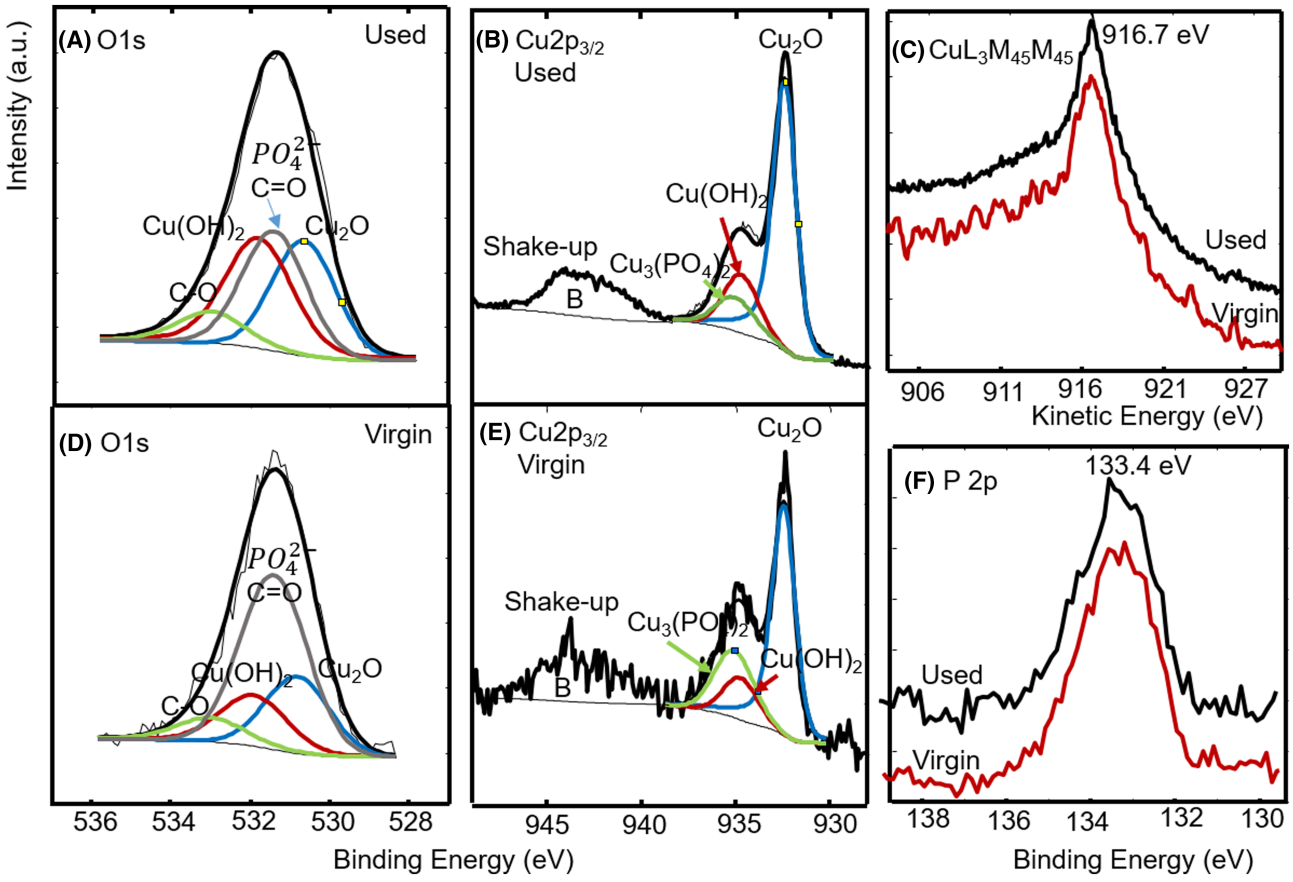

FIGURE 4 XPS core level spectra of Cu $2p_{3/2}$, O 1s and Auger Cu $L_3M_{45}M_{45}$ peaks of virgin and used 99.70% Cu

nm to 30 nm) and an increase of oxygen content by 180 ppm. The corresponding values for the 99.95 grade were ~13 nm (from 2 nm to 15 nm) and 295 ppm oxygen, respectively. For these two powder having similar size distribution, the increase of the oxide thickness differed by only 15% for the reused condition, while the oxygen up-take differed by 39%. This could be explained by the fact that the oxide formed during recycling was mainly Cu_2O for the 99.70 grade powder while it was a mixture of Cu_2O and CuO, with a considerable increased fraction of CuO for the 99.95 grade. Clearly, less O was contained in Cu_2O, leading to slower rate of oxygen up-take in the case of low purity grade.

4 | CONCLUSIONS

The surface oxide characteristics before and after repeated usage in the LPBF process were examined for two different pure Cu powder grades, one grade designated as 99.95% purity and one designated as 99.70% purity. A clear difference between the two powder grades was observed.

The surface oxides on 99.95% powder consisted of Cu_2O, CuO and $Cu(OH)_2$, and recycling increased the fraction of CuO considerably. In the case of low purity powder, Cu was mainly in the chemical state of $Cu(OH)_2$, Cu_2O and $Cu_3(PO_4)_2$ while CuO was not formed anymore. Surface enrichment of phosphorus as phosphate was hence depicted for the 99.70% grade in virgin condition, but the relative surface quantity was decreased when exposed in the LPBF process. The overall oxide thicknesses depended on grade and condition. Both powder grades showed extensive increase in the oxide thickness and total oxygen pick-up as a result of being repeatedly exposed in the LPBF process. The thinnest oxide thickness of 2 nm was shown for virgin 99.95% grade powder, and the greatest thickness of 30 nm was found for the used 99.70% grade powder. The bulk oxygen content levels showed the same trends, though the speed of oxygen up-take was slower for the 99.70% powder due to the formation of less oxygen containing oxide Cu_2O.

ACKNOWLEDGEMENTS

The authors are grateful for the collaborative efforts from the project partners and the funding from Swedish Agency for Innovation Systems (Vinnova) via the strategic innovation programme Production2030 as well as the European Union—European Structural and Investment Funds administrated by Swedish Agency for Economic and Regional Growth and Västra Götalandsregionen. Special thanks are extended to EOS Oy for providing the copper powder samples used and their technical co-operation.

ORCID

Eric Bojestig https://orcid.org/0000-0003-1057-6479
Yu Cao https://orcid.org/0000-0002-1965-5854
Lars Nyborg https://orcid.org/0000-0002-1726-5529

REFERENCES

1. Frazier WE. Metal additive manufacturing: a review. *J Mater Eng Perform*. 2014;23(6):1917-1928. https://doi.org/10.1007/s11665-014-0958-z
2. Saunders M. X marks the spot—find the ideal process parameters for your metal AM parts.; 2017. https://resources.renishaw.com/en/details/%2010%2010106810
3. Vock S, Klöden B, Kirchner A, Weißgärber T, Kieback B. Powders for powder bed fusion: a review. *Prog Addit Manuf*. February 2019;4(4):1-15. https://doi.org/10.1007/s40964-019-00078-6
4. Cordova L, Campos M, Tinga T. Revealing the effects of powder reuse for selective laser melting by powder characterization. *JOM*. 2019;71(3):1062-1072. https://doi.org/10.1007/s11837-018-3305-2
5. Olakanmi EO, Cochrane RF, Dalgarno KW. A review on selective laser sintering/melting (SLS/SLM) of aluminium alloy powders: processing, microstructure, and properties. *Prog Mater Sci*. 2015;74:401-477. https://doi.org/10.1016/j.pmatsci.2015.03.002
6. Ardila LC, Garciandia F, González-Díaz JB, et al. Effect of IN718 recycled powder reuse on properties of parts manufactured by means of selective laser melting. *Phys Procedia*. 2014;56:99-107. https://doi.org/10.1016/j.phpro.2014.08.152
7. Quinn P, O'Halloran S, Lawlor J, Raghavendra R. The effect of metal EOS 316L stainless steel additive manufacturing powder recycling on part characteristics and powder reusability. *Adv Mater Process Technol*. 2019;5(2):348-359. https://doi.org/10.1080/2374068X.2019.1594602
8. European Copper Institute. Copper as electrical conductive material with above-standard performance properties. http://www.conductivity%2010app.org/single%2010article/cu%2010overview#L13. Published 2012. Accessed October 4, 2019.
9. Ikeshoji T-T, Nakamura K, Yonehara M, Imai K, Kyogoku H. Selective laser melting of pure copper. 3AD:103–127. https://doi.org/10.1007/s11837-017-2695-x
10. Industrial Laser Solutions Editors. Green light-enabled SLM process to allow additive manufacturing of copper industrial laser solutions. https://www.industrial%2010lasers.com/additive%2010manufacturing/article/16490235/green%2010lightenabled%2010slm%2010process%2010to%2010allow%2010additive%2010manufacturing%2010of%2010copper. Published 2017. Accessed October 4, 2019.
11. Lykov P, Baytimerov R, Vaulin S, Safonov E, Zherebtsov D. Selective laser melting of copper by 200 W CO2 laser. In: 2016. https://doi.org/10.4271/2016-01-0333
12. Colopi M, Caprio L, Demir AG, Previtali B. Selective laser melting of pure Cu with a 1 kW single mode fiber laser. *Procedia CIRP*. 2018;74:59-63. https://doi.org/10.1016/J.PROCIR.2018.08.030
13. CS/ONH-analysis—elemental analysis, combustion analyzers, hydrogen analyzers—X-ray diffraction and elemental analysis|Bruker. https://www.bruker.com/products/x%2010ray%2010diffraction%2010and%2010elemental%2010analysis/csonh%2010analysis.html?campaign=CS%2010ONH%2010US%2010Canada%26gclid=EAIaIQobChMIptSns%2010eN6QIVicx3Ch3_BAp_EAAYASAAEgK86vD_BwE. Accessed April 29, 2020.
14. Biesinger MC. Advanced analysis of copper X-ray photoelectron spectra. *Surf Interface Anal*. 2017;49(13):1325-1334. https://doi.org/10.1002/sia.6239
15. Lee MY, Ding SJ, Wu CC, Peng J, Jiang CT, Chou CC. Fabrication of nanostructured copper phosphate electrodes for thedetection of α-amino acids. *Sens Actuators B*. 2015;206:584-591. https://doi.org/10.1016/j.snb.2014.09.106
16. Rotole JA, Sherwood PMA. Oxide-free phosphate films on copper probed by core and valence-band x-ray photoelectron spectroscopic studies in an anaerobic cell. *J Vac Sci Technol a Vacuum, Surfaces, Film*. 2000;18(4):1066-1071. https://doi.org/10.1116/1.582301

17. Dang H, Cao L, Li J, et al. Controlling the thickness of amorphous layer on $Cu_3(PO4)_2$ particle for promoted sodium storage reversibility as a conversion-reaction-based cathode. *J Electroanal Chem*. 2019;852:113406. https://doi.org/10.1016/j.jelechem.2019.113406
18. Magnusson H, Lindberg F, Frisk K. Validating thermodynamic description of copper oxides and phosphates by controlled oxidation of OFP-copper.; 2015. https://skb.se/publikation/2485262/R-15-06.pdf. Accessed April 30, 2020.

How to cite this article: Bojestig E, Cao Y, Nyborg L. Surface chemical analysis of copper powder used in additive manufacturing. *Surf Interface Anal*. 2020;52:1104–1110. https://doi.org/10.1002/sia.6833